Vlgr1 is required for proper stereocilia maturation of cochlear hair cells

Hideshi Yagi[1,2], Hisashi Tokano[3], Mitsuyo Maeda[4], Tetsuji Takabayashi[1,5], Takashi Nagano[1], Hiroshi Kiyama[4], Shigeharu Fujieda[5], Ken Kitamura[3] and Makoto Sato[1,2,6,*]

[1]*Division of Cell Biology and Neuroscience, Department of Morphological and Physiological Sciences,* [2]*Research and Education Program for Life Science, University of Fukui, Fukui 910-1193, Japan*

[3]*Department of Otolaryngology, Tokyo Medical and Dental University, Tokyo 113-8519, Japan*

[4]*Department of Anatomy and Neurobiology, Graduate School of Medicine, Osaka City University, Osaka 545-8585, Japan*

[5]*Division of Otorhinolaryngology, Department of Sensory and Locomotor Medicine, Faculty of Medical Sciences, University of Fukui, Fukui 910-1193, Japan*

[6]*Solution Oriented Research for Science and Technology (SORST), Japan Science and Technology Agency (JST), Kawaguchi, Saitama 332-0012, Japan*

Very large G-protein coupled receptor (Vlgr1b) is the largest known G-protein coupled receptor. Its function is unknown, although mice with deletion of Vlgr1 (Vlgr1b together with other splicing variants, Vlgr1c, Vlgr1d and Vlgr1e) are known to exhibit audiogenic seizure susceptibility and *VLGR1* is reported to be the gene responsible for Usher type 2C syndrome. We demonstrated here that *Vlgr1*-mutated mice suffered from a hearing defect because of inner ear dysfunction, as indicated by auditory brainstem response (ABR) and distortion product oto-acoustic emissions (DPOAE). The expression of Vlgr1 was identified in the developing hair cells perinatally, and the translated products were seen to be localized in the base of stereocilia on hair cells using confocal microscopy. This Vlgr1 localization was limited to the base of stereocilia within approximately 200–400 nm from the apical surface of hair cells, as shown by immunoelectron microscopy. The *Vlgr1*-mutated mice exhibited malformation of the stereocilia; the cochlear hair bundles were apparently normal at birth but then became disarranged at postnatal day 8. Furthermore, the stereocilia in the mutant mice became slanted and disarranged thereafter. These results indicate that loss of Vlgr1 resulted in abnormal development of stereocilia formation.

Introduction

Deafness occurs in approximately 1 out of 1000 people in the United States and United Kingdom, and effective methods for the treatment and prevention of deafness need to be developed, and will depend on clarifying the hearing processes and their underlying molecular mechanisms (Hone & Smith 2001; Bitner-Glindzicz 2002; Nance 2003). In the complicated hearing pathways, the transduction of acoustic stimuli into electrical signals is a very unique system for sensing sounds, and molecules that are engaged in this transduction are encoded by potential "deafness genes," whose mutations cause hearing impairment. Hair cells in the cochlea of the inner ear are transducer cells, of which there are two types: outer hair cells and inner hair cells. The outer hair cells function as sensory-effector cells that augment the motion of the basilar membrane at low sound pressure levels and decrease it at high levels, while the inner hair cells work mainly as receptors for sound. These hair cells are columnar cells that have bundles of protrusions called stereocilia. Stereocilia are organized in rows with increasing height to form the staircase-like shape of a hair bundle. This staircase-like shape is important to make the tip link that is considered to act as a gate for the transduction channel (Denk *et al.* 1995). Stereocilia are also formed in the hair cells of the vestibule, where they sense balance and acceleration.

So far, most molecules that have been shown to be related to stereocilium development have been recognized as being encoded by "deafness genes." Several intracellular

Communicated by: Yoshimi Takai

**Correspondence*: E-mail: makosato@fmsrsa.fukui-med.ac.jp

DOI: 10.1111/j.1365-2443.2007.01046.x

motor and intercellular adhesion molecules have been implicated in stereocilium morphogenesis (Frolenkov *et al.* 2004). The intercellular adhesion molecules involved in stereocilium morphogenesis play roles in hair bundle formation; for example, protocadherin 15 is thought to maintain the connections between stereocilia (Ahmed *et al.* 2003). Ultrastructural studies have uncovered four different types of links between stereocilia, some of which are assumed to provide cohesiveness to the stereocilia bundles and to mediate signaling events during morphogenesis (Frolenkov *et al.* 2004). Among the four links, the ankle link, by which the bases of stereocilia are connected, appears only for a short time during the postnatal period during development, and its role in the formation of stereocilia and its relationship to their constituent molecules remain unknown (Frolenkov *et al.* 2004).

Usher syndromes, whose features include congenital hearing loss and retinitis pigmentosa, are genetically heterogeneous autosomal recessive disorders (Keats & Corney 1999). Among the three clinically distinguishable types of Usher syndromes, Usher type 2 shows moderate to severe high frequency hearing loss and normal vestibular function. Genetic studies have resulted in subgrouping Usher type 2 patients into three types, Usher type 2A, 2B and 2C. Among them, Usher type 2C patients have been shown to have atrophic changes in the organ of Corti, and mutations in the very large G-protein coupled receptor 1 ((*VLGR1*), also named MGR1) locus (also called the mass1 locus) are highly likely to be involved in the pathogenesis of Usher type 2C syndrome (Weston *et al.* 2004). Several splicing variants are transcribed from the *Vlgr1* locus, the longest of which is Vlgr1b (McMillan *et al.* 2002; Yagi *et al.* 2005). Vlgr1b, whose mRNA is approximately 19 kb in size, is one of the G-protein coupled receptors with a huge extracellular domain in which there are many Calx-β domains, potential calcium binding domains, as inferred from the deduced amino acid sequence. We identified two alternative splicing variants, Vlgr1d and Vlgr1e, and made *Vlgr1* knockout mice that lost the functional products of Vlgr1b, Vlgr1d, Vlgr1e and Vlgr1c, which is another alternative splicing variant of Vlgr1 (McMillan *et al.* 2002; Yagi *et al.* 2005). Mass1, which is one of the Vlgr1 alternative splicing variants, was reported to be the gene responsible for the susceptibility to audiogenic seizure of Frings mice (Skradski *et al.* 2001). Frings mice carry a spontaneous mutation of Mass1 (*Mass1*^{Frings}) that also results in mutation of Vlgr1b (McMillan *et al.* 2002). Then, we and other groups observed that *Vlgr1* (Vlgr1b, Vlgr1c, Vlgr1d, Vlgr1e) knockout mice and mice with mutated *Vlgr1* show high susceptibility to audiogenic seizures (Skradski *et al.* 2001; Yagi *et al.* 2003, 2005; McMillan & White 2004). Recently, cochlear abnormalities were reported in BUB/BnJ mice, which carry a *Mass1*^{Frings} type mutation and a mutation of *cadherin 23*, also known as age-related hearing loss (*ahl*) (Johnson *et al.* 2000, 2005; Noben-Trauth *et al.* 2003) and in Vlgr1/del7TM mice, in which the transmembrane domain of Vlgr1 is deleted (McGee *et al.* 2006).

In the study presented here, we found that Vlgr1 was expressed in the base of stereocilia where and when the ankle link is formed. We then demonstrated that deletion of Vlgr1 resulted in hearing impairment and distorted stereocilia development.

Results

Vlgr1 was expressed in the hair cells of the inner ear

In order to examine in detail the regions where Vlgr1 is expressed, *Vlgr1-EYFP* (enhanced yellow fluorescent protein) knock-in mice, which express EYFP following the first 15 amino acid residues of Vlgr1, instead of full-length Vlgr1, were generated (Fig. 1A). In order to detect EYFP signals as sensitively as possible, we performed immunohistochemical detection using anti-green fluorescent protein (GFP) antisera (Tamamaki *et al.* 2000) in order to identify regions with expression of the EYFP protein. In the *Vlgr1-EYFP* knock-in mice, EYFP expression was confirmed in the ventricular zone, where the Vlgr1 mRNA is known to be expressed, at embryonic day 14 (E14) (Fig. 1B) (Yagi *et al.* 2005). The expression of EYFP was observed in the sensory epithelium of the auditory vesicle at E14 in the *Vlgr1-EYFP* knock-in mice (Fig. 1D). EYFP expression in the cochlea was confined to the inner and outer hair cells at P0 (Fig. 1E). This restricted expression was confirmed by immunohistochemical staining for Math1, which is a marker for the hair cells in the inner ear (Fig. 1F) (Bermingham *et al.* 1999). Hair cells in the macula of the saccule, the macula of the utricle and the ampullary crest also expressed EYFP at P0 (data not shown). EYFP expression in the hair cells of the inner ear decreased as development proceeded: it was very weak at P8, and was nearly undetectable in the adult (unpublished data).

Vlgr1 expression was limited to the base of stereocilia and Vlgr1 was involved in the ankle link of stereocilia

To investigate the subcellular localization of Vlgr1, we raised antisera against the N-terminal region of Vlgr1. Immunohistochemical analysis with our antisera showed that Vlgr1 was expressed in the hair cells of the cochlea and vestibule of wild-type mice at P0. The expression of

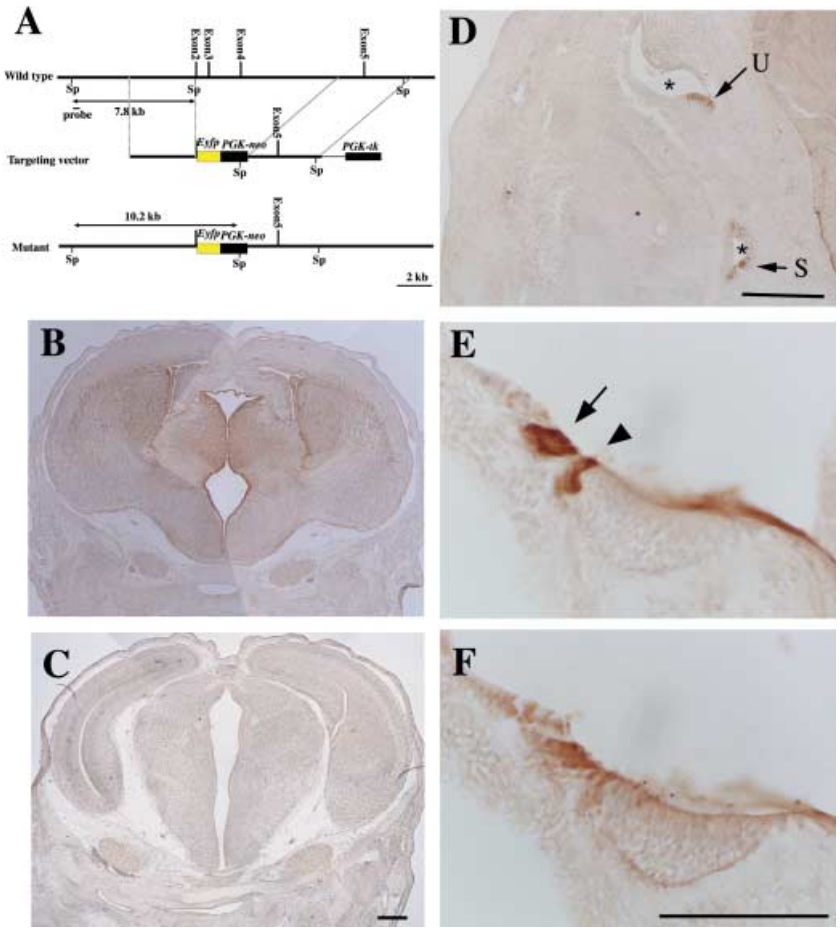

Figure 1 Vlgr1 is expressed in the hair cells of inner ear. (A) Maps of the targeting vector, wild-type allele, and mutant allele of *Vlgr1-EYFP* knock-in mice. Sp indicates the restriction enzyme site of *Spe*I. (B)–(F) EYFP expression was visualized with anti-GFP antisera using immunohistology. (B, C) Coronal section of *Vlgr1-EYFP* knock-in mouse (B) and wild-type littermate (C) at E14. Scale bar = 100 μm (shown in (C)) (D) Otic vesicle of *Vlgr1-EYFP* knock-in mouse at E14. Asterisks show otic vesicle. Brown signals located on the sensory epithelia of the utricle (U) and the saccule (S). Scale bar = 100 μm. (E) Cochlea of *Vlgr1-EYFP* knock-in mouse at postnatal day 1. An arrow indicates the outer hair cells. An arrowhead indicates the inner hair cell. (F) Using anti-math1 antisera, Math1 expression was detected in the section adjacent to that shown in (E) in the same region as Vlgr1-expressing cells observed in (E). Scale bar = 100 μm.

Vlgr1 was localized in the hair bundles of hair cells at P0. In the cochlea, the expression of Vlgr1 was observed in the hair bundles of hair cells localized from the apical to basal turn of the cochlea (Fig. 2A). Double labeling with phalloidin indicated that the region immunopositive for Vlgr1 was the base of the hair bundles (Fig. 2B). No such immunoreactivity was recognized in the *Vlgr1-EYFP* knock-in mice or our *Vlgr1* knockout mice, in which expression of Vlgr1b mRNA was not detected (Yagi *et al.* 2005). Since there was no detectable difference between these two kinds of mice in the subsequent histological and physiological tests (unpublished data), these two types of mice are called *Vlgr1*-mutated mice hereafter. Vlgr1 expression was also observed at the base of hair bundles from the apical to basal turn of the cochlea at P8 (Fig. 2C,D). We observed that the expression of Vlgr1 was localized at the base of stereocilia and between the stereocilia (Fig. 2E–J). At the same time, the expression of Vlgr1 was observed at the base of the hair bundles of the vestibular hair cells at P2 and P8. During postnatal development, the expression of Vlgr1 was almost undetectable at P12. We further studied the expression of Vlgr1 during various embryonic stages. At E16, faint expression of Vlgr1 was recognized in the cochlear hair cells with our antisera against Vlgr1 (data not shown). At E18, expression of Vlgr1 was clearly observed in the hair cells at the basal turn of the cochlea with the same antiserum, while the hair cells from the mid to apical turn of the cochlea were not noticeably immunopositive (data not shown). The immunoelectron microscopy was employed in order to investigate the expressed portion of Vlgr1. The immunoreactivity was observed on the stereocilia 200–400 nm above the apical surface of cochlear outer hair cells at P2 (Fig. 2K,L). We also observed the immunoreactivity of anti-Vlgr1 antisera at almost the same position at P8 (data not shown). We further studied the relationship between ankle links and Vlgr1, since it was reported that ankle links disappear under calcium-free conditions (Goodyear & Richardson 1999). After normal mice cochleae were incubated in Hanks' balanced salt

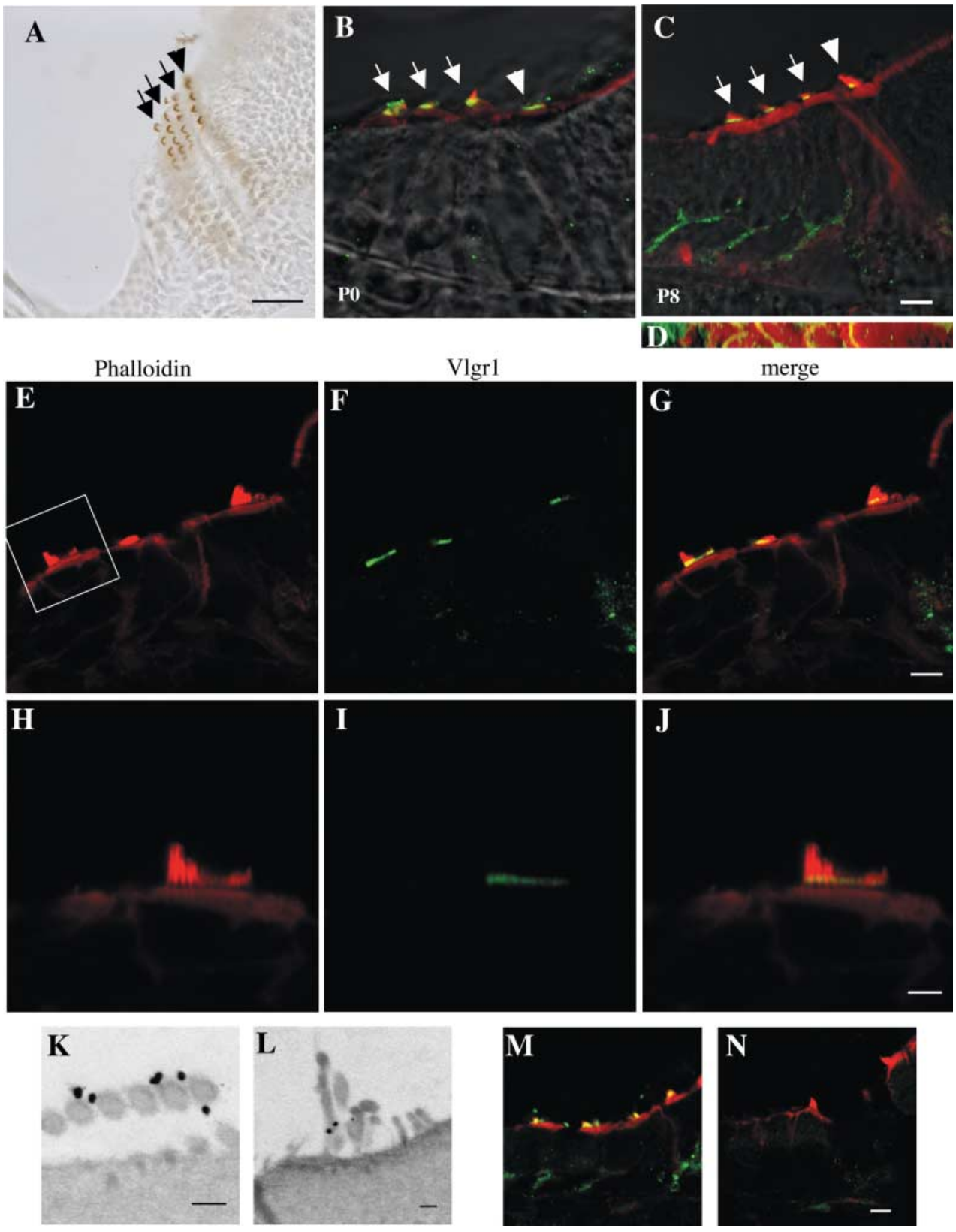

solution without calcium or magnesium ion (HBSS(-)) and in the HBSS(-) containing 5 mM 1,2-bis(2-aminophenoxy)ethane-*N*, *N*, *N*′, *N*′-tetraacetic acid tetrapotassium salt (BAPTA) for 1 h. The Vlgr1 expression was limited to the base of hair bundles in cochlea incubated with HBSS(-) (Fig. 2M), while the Vlgr1 expression vanished after incubation with HBSS(-) containing 5 mM BAPTA (Fig. 2N).

Cochlea function of the *Vlgr1*-mutated mice was impaired

The strong expression of Vlgr1 in the hair cells of the developing inner ear prompted us to examine the role of Vlgr1 in inner ear function. First, the hearing ability of *Vlgr1*-mutated mice was investigated using the auditory brainstem response (ABR) method. The mean ABR threshold of postnatal 3-week-old *Vlgr1*-mutated mice was elevated to approximately 80 dB (Fig. 3B), while those of their wild-type littermates and heterozygous mice were approximately 20–30 dB at 8 kHz (Fig. 3A). There was no significant difference between males (92.5 dB, $n = 4$) and females (88.8 dB, $n = 8$) in the ABR threshold. This indicates that the hearing ability is impaired in the *Vlgr1*-mutated mice. The hearing ability of the *Vlgr1*-mutated mice was further studied at an older age, 2 months old, at various frequencies, and consistent results were observed (Fig. 3C). The average ABR threshold of *Vlgr1*-mutated mice at 8 kHz was 93.3 kHz ($n = 3$) at around 1-year-old. By contrast, the latencies of the wave peaks of the ABR were similar among the homozygous *Vlgr1*-mutated mice, their wild-type littermates and heterozygous mice (Fig. 3A,B), suggesting that auditory information was properly transmitted from the inner ear to the brain in all cases tested. Since the results obtained by the ABR method indicated malfunction of the inner ear, we examined whether the cochlea function was impaired in the 2-month-old *Vlgr1*-mutated mice or not by performing the distortion product oto-acoustic emission test (DPOAE), in which the acoustic emission at a specific frequency ($2f_2–f_1$) from the inner ear is measured while exposing mice to two frequencies, f_1 and f_2, simultaneously. A marked level of emission is detected if the function of the outer hair cells is not impaired. The mean emission levels of the *Vlgr1*-mutated mice were within the background noise level, while levels closer to the normal emission levels were detected for the heterozygous mice (Fig. 3D). The results obtained by the ABR method and DPOAE indicated that the cochleae, particularly the outer hair cells, of *Vlgr1*-mutated mice were malfunctional.

Outer hair cells of the cochlea were lost in the adult *Vlgr1*-mutated mice

The transient perinatal expression of Vlgr1 in the hair cells suggested the involvement of Vlgr1 in the development of hair cells in the cochlea. However, no apparent histological abnormalities were observed in the cochlea of P25 *Vlgr1*-mutated mice by hematoxylin-eosin staining (Fig. 4B,D). Proper arrangement of the hair cells, one row of inner hair cells and three rows of outer hair cells, was observed in the *Vlgr1*-mutated mice at P25 (Fig. 4D). However, some outer hair cells were lost at the basal turn in the organ of Corti of approximately 2-month-old *Vlgr1*-mutated mice (Fig. 4H). Such hair cell loss progressed from the bottom to the apical of the cochlea with the advancement of age (Fig. 4L). We estimated the number of missing hair cells using whole-mount preparations of cochlea. The apparent outer hair cell loss was not observed until P27 in *Vlgr1*-mutated mice (Table 1). In the wild-type and heterozygous littermates, approximately 90% of hair cells were observed even at 1-year-old (Table 1). In around 2-month-old *Vlgr1*-mutated mice, approximately 50% of outer hair cells were lost at the basal turn of the cochlea, whereas at the mid and apical turns of the cochlea, the outer hair cell loss was less than 10% of counted hair cells (Table 1). At one year old, approximately 50% outer hair cell loss was observed at the apical turn of the cochlea and over

Figure 2 Vlgr1 was expressed in the basal side of stereocilia. (A) Normal cochlea of postnatal day 0. Immunoreactivity against Vlgr1 was visualized using DAB reaction. Arrows indicate the lines of outer hair cells and an arrowhead indicates the line of inner ear cells. Scale bar = 50 μm. (B) Normal cochlea of postnatal day 0. Arrows indicate the outer hair cells and an arrowhead indicates the inner ear cell. (C) Normal cochlea of postnatal day 8. On the top of three outer hair cells (arrows) and one inner hair cell (arrowhead), stereocilia were visualized using phalloidin, and immunoreactivity of Vlgr1 could be observed at the base of stereocilia. (D) Top view of cochlea that was reconstituted from compiled confocal images including Fig. 2C. Scale bar = 5 μm shown in (C) for (B)–(D). (E–G) Normal cochlea of postnatal day 8. Scale bar = 5 μm shown in (G). (H–J) Highly magnified view of square shown in Fig. 2E. Scale bar = 2 μm shown in (J). (K, L) Immunoelectron microscope images of stereocilia on outer hair cell at P2. Scale bar = 200 nm. (M, N) The immunoreactivity of Vlgr1 vanished from the base of hair bundles with treatment with BAPTA. Compared with the control (M), 5 mM BAPTA treatment (N) completely abolished the immunoreactivity of Vlgr1 at P2. Scale bar = 5 μm. (B–J, M, N) Actin filaments were visualized using Alexa Fluor 568 phalloidin (red). Immunoreactivity against Vlgr1 was visualized using goat anti-rabbit IgG Alexa Fluor 488 (green).

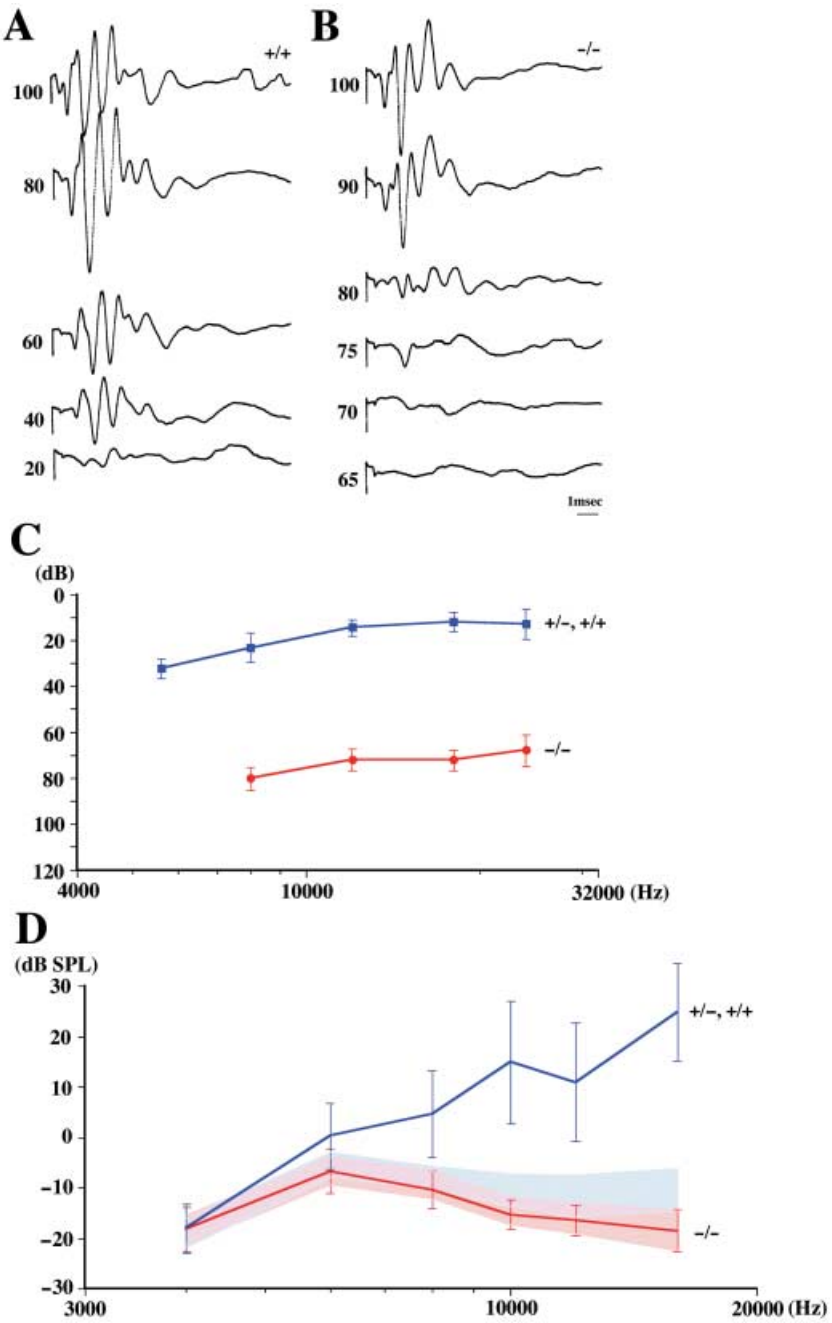

Figure 3 Vlgr1 mutant mice showed a hearing defect. (A) Auditory brainstem response (ABR) pattern of 3-week-old normal littermate of a *Vlgr1*-mutated mouse induced by 8 kHz tone at 100, 80, 60, 40, 30 and 20 dB. (B) ABR pattern of a 3-week-old *Vlgr1*-mutated mouse induced by 8 kHz tone at 100, 90, 80 and 70 dB. (C) Average ABR threshold for 2-month-old *Vlgr1*-mutated mice (n = 12) and their littermates (n = 13). These data were obtained from bilateral ears. The blue line shows the ABR threshold of control mice consisting of normal and heterozygous mice (+/–, +/+). The red line shows the ABR threshold of *Vlgr1*-mutated mice (–/–). At 5.6 kHz, the ABR threshold of *Vlgr1*-mutated mice was over 90 dB. The results represent the mean ± standard deviation (SD). (D) Mean emission levels of DPOAE for *Vlgr1*-mutated mice (red line, –/–) and their normal and heterozygous littermates (blue line, +/–, +/+). The data were obtained from 12 *Vlgr1*-mutated mice and 13 of their normal and heterozygous littermates. The pale red area and pale blue area show mean noise levels ± SD of *Vlgr1*-mutated mice and their normal and heterozygous littermates.

80% of the outer hair cells were lost at the mid turn of the cochlea in *Vlgr1*-mutated mice (Table 1).The inner hair cells of the *Vlgr1*-mutated mice were retained well compared to the outer hair cells of the *Vlgr1*-mutated mice (Table 1). Furthermore, the spiral ganglion neurons and nerve bundles under the sensory epithelium of the cochlea were missing at the basal turn of the cochlea in 12-month-old *Vlgr1*-mutated mice (Fig. 4J). By contrast, there were no apparent abnormalities in the morphology of the stria vascularis in the cochleae of *Vlgr1*-mutated mice.

Stereocilia were not properly developed in the *Vlgr1*-mutated mice

Since no apparent malformation was observed in the cochlea of the *Vlgr1*-mutated mice by hematoxylin-eosin

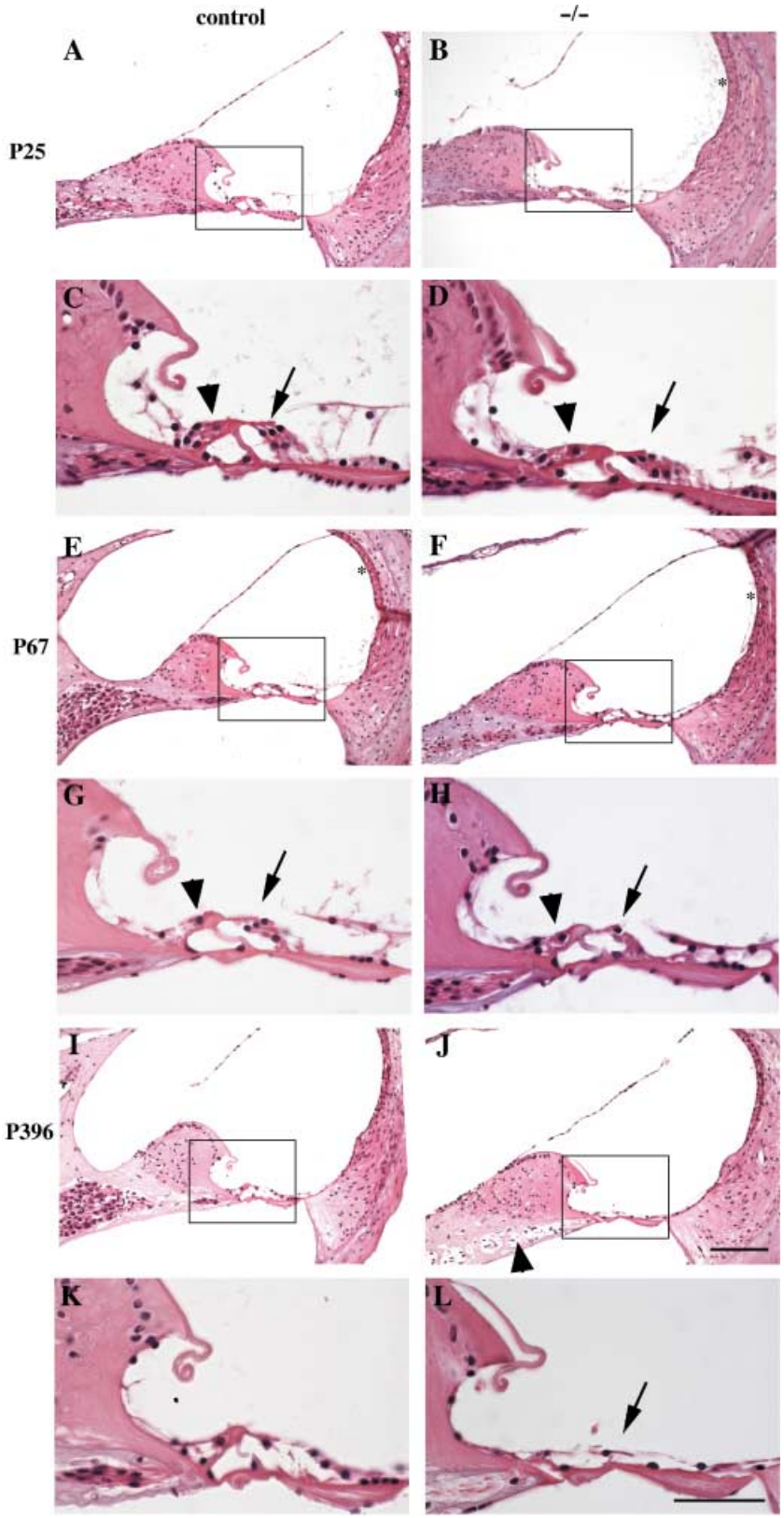

Figure 4 Organ of Corti of *Vlgr1*-mutated mice degenerated with the advance of age. (A–D) The morphology of the organ of Corti of *Vlgr1*-mutated mice could not be distinguished from that of control littermates at postnatal day 25. Squares shown in (A, B, E, F, I, J) were magnified and shown in (C, D, G, H, K, L). (A) The morphology of the basal turn of cochlea of the heterozygous littermate of a *Vlgr1*-mutated mouse. (B) The morphology of the basal turn of cochlea of a *Vlgr1*-mutated mouse. (C) High magnification of (A). (D) High magnification of (B). An arrow indicates the outer hair cells and an arrowhead indicates the inner hair cell. (E–H) At postnatal day 67, some outer hair cells of *Vlgr1*-mutated mice were lost. (E) The basal turn of the cochlea of the heterozygous littermate of a *Vlgr1*-mutated mouse. (F) The basal turn of the cochlea of a *Vlgr1*-mutated mouse. (G) High magnification of (E). An arrow indicates the outer hair cells and an arrowhead indicates the inner hair cells. (H) Higher magnification of (F). An arrow indicates the outer hair cells and an arrowhead indicates the inner hair cells. (I–L) At postnatal day 396, almost all of the cells of the organ of Corti (arrow) of *Vlgr1*-mutated mice and their nerve fibers (arrowhead) were lost. (I) The basal turn of the cochlea of a wild-type littermate. (J) The basal turn of the cochlea of a *Vlgr1*-mutated mouse. (K) High magnification of (I). (L) High magnification of (J). Asterisks indicate the stria vascularis. (A, B, E, F, I, J) Scale bar = 100 μm (shown in (J)). (C, D, G, H, K, L) Scale bar = 50 μm (shown in (L)).

Table 1 Number of missing hair cells

		Apical turn		Mid turn		Basal turn	
	Number of tested mice	Number of observed cells	Number of lost cells	Number of observed cells	Number of lost cells	Number of observed cells	Number of lost cells
Outer hair cells							
P27 control	$n = 1$	72	2 (2.8)	162	0 (0)	123	1 (0.8)
P27 −/−	$n = 4$	366	13 (3.6)	570	4 (0.7)	396	2 (0.5)
P58 control	$n = 1$	90	0 (0)	87	0 (0)	93	1 (1.1)★
P58 −/−	$n = 3$	209	2 (0.1)	570	16 (2.8)	279	123 (44.1)★
P102 control	$n = 3$	261	1 (0.3)	395	2 (0.5)★	192	2 (1.0)★
P102 −/−	$n = 3$	261	2 (0.8)	412	85 (20.6)★	371	209 (56.3)★
1-year-old control	$n = 2$	162	15 (9.3)★	144	2 (1.4)★	87	2 (2.3)
1-year-old −/−	$n = 2$	186	89 (47.8)★	78	65 (83.3)★	n.d.	n.d.
Inner hair cells							
P27 control	$n = 1$	32	0 (0)	52	0 (0)	15	0 (0)
P27 −/−	$n = 4$	118	0 (0)	209	0 (0)	128	1 (0.8)
P58 control	$n = 1$	31	0 (0)	28	0 (0)	20	0 (0)
P58 −/−	$n = 3$	81	0 (0)	183	0 (0)	115	1 (0.9)
P102 control	$n = 3$	64	0 (0)	106	0 (0)	52	0 (0)★
P102 −/−	$n = 3$	88	0 (0)	144	5 (3.5)	109	25 (22.9)★
1-year-old control	$n = 2$	20	1 (5.0)	36	2 (5.6)	20	0 (0)★
1-year-old −/−	$n = 2$	61	2 (3.3)	26	5 (19.2)	25	12 (48.0)★

Figures in parentheses indicate the percentages of lost cells relative to total observed cells. Control means wild-type and heterozygous littermates and −/− means *Vlgr1*-mutated mice. "n.d." means that the structures of the organ of Corti were damaged and the number of hair cells could not be counted. Asterisks indicate that there is a statistical difference ($P < 0.01$) between the control and −/−.

staining at P25, we further studied the development of the hair bundles of hair cells using scanning electron microscopy. At birth, the arrangements of hair bundles were not markedly abnormal in the *Vlgr1*-mutated mice (Fig. 5B,S). The kinocilium was located on the strial side of the surface of outer hair cells, and a semi-circular configuration of stereocilia characterized by a gradation in height toward the kinocilium was observed in the *Vlgr1*-mutated mice (Fig. 5D), as in their heterozygous littermates (Fig. 5C). At P4, hair bundles of the outer hair cells formed regular V or W shapes in the heterozygous littermates (Fig. 5E), while those of *Vlgr1*-mutated mice

Figure 5 Hair bundles of outer hair cells in *Vlgr1*-mutated mice were disoriented. (A, B) Scanning electron micrographs of apical surfaces of the organ of Corti located in mid-turn of cochlea dissected out from normal littermate (A) and *Vlgr1*-mutated mouse (B) at postnatal day 0. (C) High magnification of (A). (D) High magnification of (B). Arrows indicate the kinocilium. (E, F) Scanning electron micrographs of apical surfaces of the organ of Corti located in mid-turn of cochlea dissected out from heterozygous mouse (E) and *Vlgr1*-mutated mouse (F) at postnatal day 4. (G) High magnification of (E). (H) High magnification of (F). (I, J) Scanning electron micrographs of apical surfaces of the organ of Corti located in the mid-turn of the cochlea dissected out from a heterozygous mouse (I) and a *Vlgr1*-mutated mouse (J) at postnatal day 8. (K) High magnification of (I). (L) High magnification of (J). (M, N) Scanning electron micrographs of apical surfaces of the organ of Corti located in the mid-turn of the cochlea dissected out from a heterozygous mouse (M) and a *Vlgr1*-mutated mouse (N) at postnatal day 15. (O, P) High magnification of the hair bundle of outer hair cells of a heterozygous mouse (O) and a *Vlgr1*-mutated mouse (P). (Q, R) Scanning electron micrographs of apical surfaces of outer hair cells dissected out from a heterozygous mouse (M) and a *Vlgr1*-mutated mouse (N) at 2 months old. (A, B, E, F, I, J, M, N) Scale bar = 5 μm (shown in (B, F, J, N)). (C, D, G, H, K, L, O, P) Scale bar = 1 μm (shown in (D, H, L, P)). (Q, R) Scale bar = 1.2 μm (shown in (N)). IH shows the row of inner hair cells. The upper side of the figures is the modiolar side and the bottom side of the figures is the strial side. (S) The ratio of normal alignment of hair bundles. The X-axis shows the age of the tested mice and the Y-axis shows the ratio of normal hair bundles to observed whole hair bundles. Asterisks indicate that there is a significant difference ($P < 0.01$).

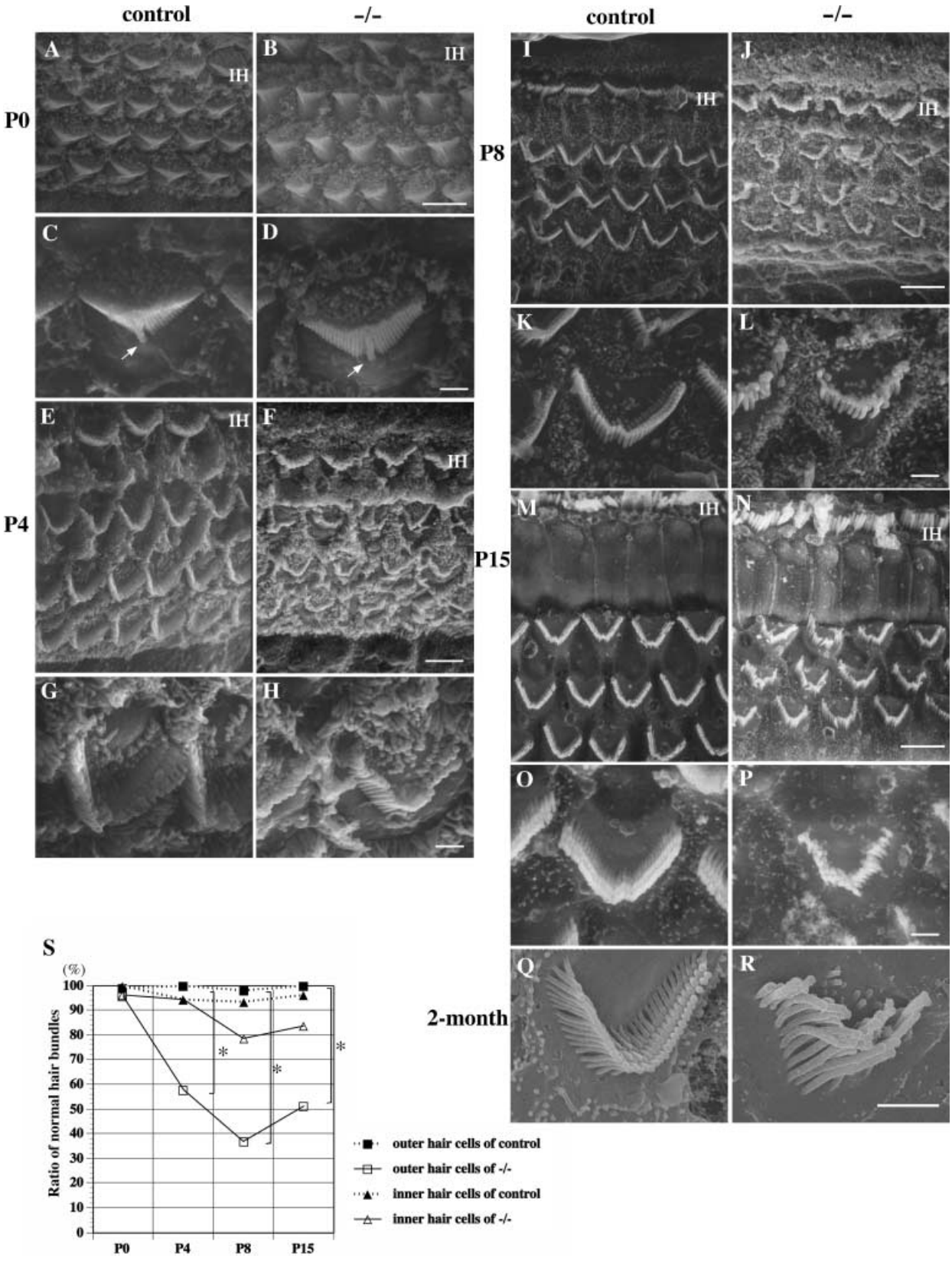

were malaligned and the hair bundles of the stereocilia on the outer hair cells were disoriented (Fig. 5F,S). Hair bundles stood on the top of the outer hair cells almost vertically, and the stereocilia of these cells were arranged in three rows with a staircase-like shape in the heterozygous littermates (Fig. 5G), whereas the stereocilia were dispersed and slanted to the modiolar side in the *Vlgr1*-mutated mice (Fig. 5H). Some stereocilia of the outer hair cells of the *Vlgr1*-mutated mice were thicker and shorter than those of control littermates. The hair bundles of the inner hair cells of *Vlgr1*-mutated mice were not so much disturbed at P4 (Fig. 5F,S). At P8, the hair bundles of the outer hair cells were disarranged in the cochleae of *Vlgr1*-mutated mice (Fig. 5J,L,S). Their stereocilia slanted toward the modiolar side to the same extent as at P4 (Fig. 5J). The hair bundles of outer hair cells in the cochlea of *Vlgr1*-mutated mice were disoriented and disarranged at P15 (Fig. 5N,S). The hair bundles of the inner hair cells of *Vlgr1*-mutated mice were not so much disturbed at P15 (Fig. 5N,S). In postnatal 2-month-old mice, the hair bundles of the outer hair cells were regular V or W shaped in the heterozygous littermates as well as in the wild-type littermates (Fig. 5Q). By contrast, the hair bundles of the outer hair cells were malaligned in the *Vlgr1*-mutated mice (Fig. 5R). The stereocilia on the top of each outer hair cell were arranged in three rows in the wild-type and heterozygous littermates, forming a staircase-like shape (Fig. 5Q), whereas the stereocilia in the homozygous *Vlgr1*-mutated mice were not arranged in a row and did not form a staircase-like shape (Fig. 5R). We further investigated the morphology of the hair bundles in the vestibular system of *Vlgr1*-mutated mice. We could not detect apparent abnormalities at the hair bundles of the maculae of the utricle and sacculus in the *Vlgr1*-mutated mice (data not shown).

The links of stereocilia were observed in *Vlgr1*-mutated mice

Transmission electron microscopy was employed to investigate the structure of the stereocilia of Vlgr1 mutated mice. The arrangement of stereocilia was regular in heterozygous littermate mice at P2 (Fig. 6A), whereas it was not regular in *Vlgr1*-mutated mice (Fig. 6B). The interstereocilial space of some regions (shown in the left half of Fig. 6B) was narrow, while that of other regions (shown in the right half of Fig. 6B) was as broad as that of heterozygous littermate mice (Fig. 6A). We further studied the interstereocilial links using transmission electron microscopy. We could observe links between

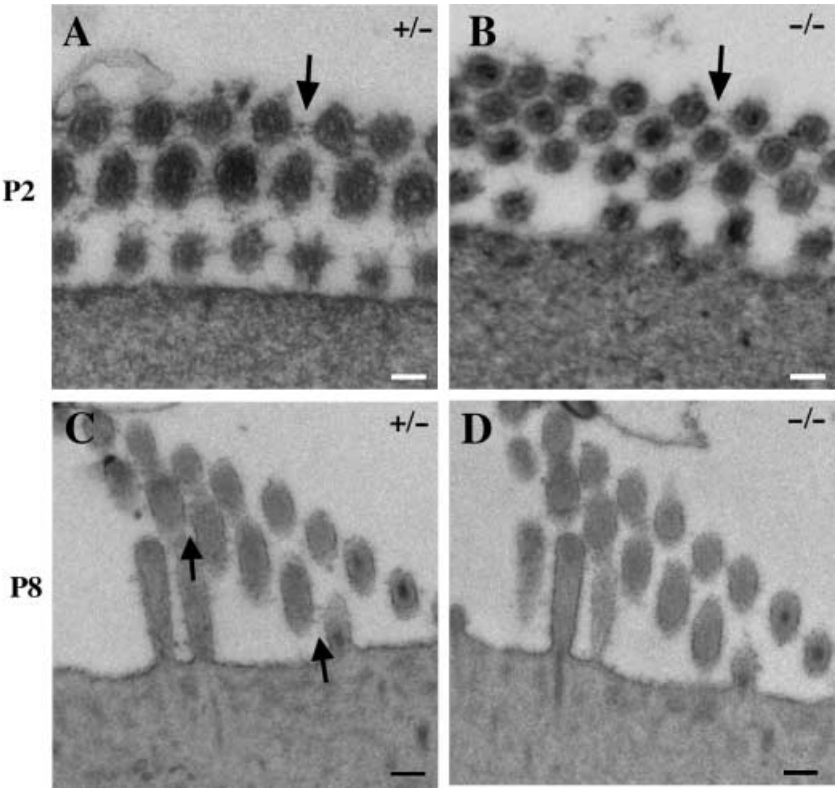

Figure 6 Interstereocilial links were not well developed in *Vlgr1*-mutated mice. (A, B) Transmission electron microscope images of stereocilia on outer hair cells of a heterozygous mice (+/–) (A) and a *Vlgr1*-mutated mice (–/–) (B) at P2. Arrows indicate interstereocilial links. Scale bar = 100 nm. (C, D) Transmission electron microscope images of stereocilia on mid-turn outer hair cell of heterozygous mice (+/–) (C) and *Vlgr1*-mutated mice (–/–) (D) at P8. Arrows indicate interstereocilial links. Scale bar = 100 nm.

the stereocilia on the outer hair cells of *Vlgr1*-mutated mice at P2 (Fig. 6B). Links were also observed between the stereocilia of heterozygous *Vlgr1*-mutated mice at P8 (Fig. 6C). Although links were sparse, we observed inter-stereocilial links between the stereocilia on the outer hair cells of *Vlgr1*-mutated mice (Fig. 6D).

There were no apparent abnormalities in the *Vlgr1*-mutated mice in the Rota-rod test

We studied the motor coordination of the *Vlgr1*-mutated mice (9–12 months old) using the Rota-rod test. The average duration until the *Vlgr1*-mutated mice dropped off the test-bar was 47.0 ± 41.0 s ($n = 6$), and the average duration until the heterozygous mice dropped off the test-bar was 53.8 ± 26.0 s ($n = 8$). There was no significant difference between homozygous and heterozygous mice ($P > 0.05$, *t*-test).

There was no apparent morphological change in the retina of *Vlgr1*-mutated mice

As Usher syndromes are characterized by congenital hearing loss and retinitis pigmentosa, we checked the retinas of *Vlgr1*-mutated mice histologically. Usually in Usher type 2, vision loss starts in the teenage years and progresses during life. We studied the eyes of 5- to 12-month-old *Vlgr1*-mutated mice. There were no apparent abnormalities in the retinas of *Vlgr1*-mutated mice. The layers of the retina were clearly identified and spontaneous fluorescence of the rods and cones was observed in *Vlgr1*-mutated mice as well as in the wild-type mice and heterozygous littermates (data not shown).

Discussion

Our finding in this study that no EYFP signals were observed in any auditory relay neurons to the inferior colliculi in *Vlgr1-EYFP* knock-in mice suggests that a defect of Vlgr1 in the inner ear, more precisely a defect of Vlgr1 in the hair cells, is responsible for the hearing impairment of *Vlgr1*-mutated mice. This is consistent with our results obtained by testing the ABR. The latency times of wave I to wave III of the ABR, which reflect the conduction through the proximal eighth nerve and caudal segment of the brainstem auditory pathway, did not differ between the *Vlgr1*-mutated and the wild-type mice (Markand 1994). This observation was further reinforced by the results of the DPOAE, which showed the malfunction of outer hair cells in *Vlgr1*-mutated mice. Ryan and Dallos reported that loss of the outer hair cells results in elevation of the 40–50 dB hearing threshold (Ryan & Dallos 1975), which is similar to the threshold elevation seen in our ABR results.

Transient expression of Vlgr1 was limited to the base of hair bundles of the hair cells in the inner ear from E18 to P8, according to our immunohistochemical results. Hair bundles develop from the late embryonic age to around P15 in the rat (Zine & Romand 1996), while auditory function is initiated at around P8 and is mature by P14 in mice (Alford & Ruben 1963; Forge *et al.* 1997). These reports indicate that the maturation of auditory function is closely related to the establishment of hair bundles and it is likely that Vlgr1 is involved in this process. The development of the hair bundles of hair cells in the cochlea is a four-step process. First, numerous precursor microvilli emerge around a single primary cilium and grow along with neighboring microvilli. Second, precursor microvilli stop elongating and increase in width, while the kinocilium migrates to the edge of the apical surface. After this step, stereocilia are locked in place. Third, nascent stereocilia elongate sequentially to form a staircase-like bundle. Finally, excess microvilli on the apical cell surface are resorbed (Kaltenbach *et al.* 1994; Zine & Romand 1996; Forge *et al.* 1997; Frolenkov *et al.* 2004). At birth, when the stereocilia are undergoing a second developmental process consisting of kinocilium movement and the organization of stereocilia into semicircular structures, no obvious disturbance of the stereocilium development was observed. In contrast, the hair bundles on the outer hair cells of *Vlgr1*-mutated mice were disturbed at P4. The fact that microvilli remained on the apical surface of the outer hair cells in *Vlgr1*-mutated mice whereas they were there only transiently in normal mice indicated that microvilli resorption was defective in the former. The staircase formation of stereocilia was also compromised and microvilli resorption was abnormal. Therefore, Vlgr1 is likely to be involved in the maturation of stereocilia, especially in the positioning of stereocilia and the formation of staircase structures by stereocilia.

The temporal pattern of Vlgr1 expression, in which Vlgr1 is localized in the base of hair bundles and is expressed during the early postnatal period, overlapped well with the pattern of the existence of the ankle link, which is observed transiently from P2 to P9 (Goodyear *et al.* 2005). As reducing the calcium level causes the disappearance of the ankle link (Goodyear & Richardson 1999), the disappearance of Vlgr1 immunoreactivity upon BAPTA treatment indicated that the extracellular domain of Vlgr1 was involved in the ankle link formation. Vlgr1 has a G-protein coupled receptor proteolytic site that is located at the extracellular domain near the transmembrane domain. Ig-Hepta, which is a member of the LNB-TM7 family (a subfamily of secretin type

receptors that includes Vlgr1), was reported to be cleaved at this G-protein coupled receptor proteolytic site (Abe *et al.* 2002). Since we observed links between the stereocilia of cochlear outer hair cells of *Vlgr1*-mutated mice at P2 and P8 and Vlgr1 has many Calx-β domains, whose function is related to calcium binding (Schwarz & Benzar 1997), we suppose that Vlgr1 was digested at the G-protein coupled receptor proteolytic site and the digested extracellular domain of Vlgr1 bound to other link formation proteins in the presence of calcium ion.

Vlgr1 was distributed in the base of stereocilia in the inner hair cells as well as the outer hair cells. However, our results of ABR tests and DPOAE show that the inner hair cells functioned in the *Vlgr1*-mutated mice, as those mice could hear sounds, whereas the outer hair cells were almost completely dysfunctional. This indicates that the requirement for Vlgr1 differs between the outer hair cells and the inner hair cells. Actually, the hair bundles on the outer hair cells were much distorted in the *Vlgr1*-mutated mice compared with those on the inner hair cells. The shape of the hair bundles on the inner hair cells is nearly linear and the hair bundles there consist of two rows of stereocilia, while the hair bundles on the outer hair cells are V- or W-shaped, and the hair bundles there consist of three rows of stereocilia. This ordered orientation of V- or W-shaped hair bundles is necessary for normal auditory perception (Yoshida & Liberman 1999). We speculate that the malformed hair bundles led to the dysfunction of outer hair cells and the dysfunction of the outer hair cells was related to the outer hair cell loss. It is also assumed that the requirement for Vlgr1 is less stringent for hair cells in the vestibule than for the outer hair cells.

Recently, a mutation of *VLGR1* was discovered in Usher type 2C patients (Weston *et al.* 2004). Usher type 2 patients suffer from a moderate loss of hearing in the lower sound frequency range and severe loss of hearing in the higher sound frequency range (Keats & Corney 1999). There have been several reports about the morphology of the cochlea of patients with Usher syndrome type 2 (Cremers & Delleman 1988; Wagenaar *et al.* 2000). These reports showed that the organ of Corti and spiral ganglia were severely degenerated in Usher syndrome type 2 aged and adult patients. There is no discrepancy between those reports and our observation that the outer hair cells were missing at an older age in *Vlgr1*-mutated mice.

BUB/BnJ mice show early onset of hearing insufficiency and abnormal hair bundle morphology of cochlear hair cells in the inner ear (Johnson *et al.* 2005). The splayed and disorganized morphologies of stereocilia in the inner ear of BUB/BnJ at P14 were similar to our results. BUB/BnJ mice have a point mutation of *cadherin 23* (*Cad23*$^{753G\rightarrow A}$), which is a cause of age-related hearing loss (*ahl*), as well as the *Mass1*^{frings} mutation, one type of spontaneous mutation of Vlgr1 (Johnson *et al.* 2005). As *cadherin 23* mutation was identified in patients with Usher syndrome type 1D (Bolz *et al.* 2001), *cadherin 23*-mutated mice are considered to be a model for Usher syndrome type 1D, in which one of the traits is profound deafness from birth (Hone & Smith 2001). Therefore, it is difficult to conclude that the abnormalities of BUB/BnJ mice are due to the mutation of *Mass1*/*Vlgr1*. Our *Vlgr1*-mutated mice have an advantage for model studies of Usher syndromes since their wild-type and heterozygous littermates have the same genetic background as the *Vlgr1*-mutated mice. These littermates of *Vlgr1*-mutated mice showed normal hearing ability and normal cochlear morphology in histological examinations even past 2 months of age. Only *Vlgr1*-mutated mice showed abnormal morphology of the inner ear. Recently, McGee *et al.* (2006) reported the morphological change of the hair cells of Vlgr1 knockout mice in which the transmembrane domain of Vlgr1 was lost. These knockout mice, in which the genomic locus of Vlgr1 retained the intact extracellular domain of Vlgr1, and our *Vlgr1*-mutated mice were different with regard to the part of the Vlgr1 protein that remained.

It was reported recently that Vlgr1b is co-localized with DFNB31, Ush2a, and Harmonin (Reiners *et al.* 2005; van Wijk *et al.* 2006). These molecules have been reported to be encoded by "deafness genes," and Ush2a, Harmonin and Vlgr1 are responsible genes for Usher syndromes. These molecules are reported to be co-localized at the inner ear and retina, especially at the synapse (Reiners *et al.* 2005; van Wijk *et al.* 2006). The localization of Vlgr1 at the synapse is observed at P26 (van Wijk *et al.* 2006). We used *Vlgr1*-mutated mice as negative controls for staining with anti-Vlgr1 antisera, and observed that the base of stereocilia was stained in normal mice but not in *Vlgr1*-mutated mice at P8 (data not shown). This result was almost the same as that reported by Reiners *et al.* (2005). In Fig. 2C, a Vlgr1-like signal was observed at the neurites under the outer hair cells. As we could observe almost the same signals in the *Vlgr1*-mutated mice, we suppose that this signal at the neurites was background signal at P8.

Experimental procedures

Animals

Animals were maintained on a 12-h (8:00 a.m. to 8:00 p.m.) light/12-h dark schedule at constant temperature and humidity and

provided with food and water *ad libitum*. The day that the presence of a vaginal plug was confirmed was defined as embryonic day 0 (E0). For pups, the day of birth was designated postnatal day 0 (P0). Before experiments, all animals were deeply anesthetized by hypothermia (for P0–P5), or by intraperitoneal injection of sodium pentobarbital (40 mg/kg). For embryos, their dams were deeply anesthetized with sodium pentobarbital (40 mg/kg). All experiments were conducted in accordance with the guidelines for animal experiments of the University of Fukui.

Construction of targeting vectors

To generate *EYFP* (enhanced yellow fluorescent protein; BD Biosciences Clontech, Palo Alto, CA) knock-in mice, a targeting vector was constructed in which *EYFP* followed the first 20 bp of exon 2 of Vlgr1 in frame and the rest of exon 2 and exons 3–4 were replaced by the *PGK-neo* cassette (Yagi *et al.* 1998). To construct the targeting vector, a *Bam*HI-*Spe*I fragment that contained 20 bp of exon 2 was ligated to the *EYFP* gene followed by the *PGK-neo* cassette. We inserted this 5′ region of exon 2-, *EYFP*-, *PGK-neo*-containing fragment, and a 5.0-kb *Sal*I-*Not*I fragment, which consisted of intron 4, exon 5 and intron 5, into the *Cla*I site and the *Sal*I-*Kpn*I site of pBluescript SK (Stratagene), respectively, in which the *Ssp*I fragment was replaced with the *PGK-tk* cassette (Yagi *et al.* 1998).

Antisera against Vlgr1

Antisera were raised against the N-terminal region (VLRGKDSDGN aa 282-291) of Vlgr1 in rabbits.

Histological examination

For histological examination, whole embryos or inner ears were fixed in 0.1 M phosphate buffer (PB) (pH 7.2) containing 4% paraformaldehyde (PFA) at 4 °C. After fixation, the cochleae were decalcified with 0.1 M PB containing 10% EDTA. For normal histological examination, the decalcified materials were dehydrated and embedded in paraffin. The inner ears were cut at 5-μm thickness with a microtome and the sections were stained using hematoxylin-eosin stain. Conventional protocol was used for immunohistochemical studies. The sections were incubated with the antibody-dilution-buffer (0.01 M phosphate buffered saline (PBS) containing 1% bovine serum albumin (BSA; Sigma-Aldrich, St. Louis, MO), 1% normal goat serum (NGS; Sigma-Aldrich) and 0.25% Triton X-100) for 30 min, and then were incubated overnight at 4 °C with rabbit anti-GFP antisera (Tamamaki *et al.* 2000) diluted 1:400, rabbit anti-Math1 antisera (Chemicon, Temecula, CA) diluted 1:200 or rabbit anti-Vlgr1 antisera diluted 1:500 in antibody-dilution-buffer. The signals were visualized with DAB using a Vectastain Elite ABC kit (Vector Laboratories, Burlingame, CA) and Histofine Simple Stain DAB solution (Nichirei, Tokyo Japan).

For fluorescent immunohistochemical staining, the sections were incubated with antibody-dilution-buffer for 30 min, and then with rabbit anti-Vlgr1 antisera diluted 1:200 overnight at 4 °C. After the sections were rinsed with 0.01 M PBS, they were incubated with Alexa Fluor 488-conjugated goat anti-rabbit IgG diluted 1 : 1000 and Alexa Fluor 568 phalloidin (Molecular Probes Inc., Eugene, OR). The images were obtained using a confocal laser scanning microscope (LSM5 Pascal, Carl Zeiss Japan, Tokyo Japan).

Wholemount preparation of cochlea

Inner ears were fixed as described above. After fixation, the cochleae were decalcified with 0.1 M PB containing 10% EDTA. The bone was removed from around membranous cochlea. Reissner's membrane was removed next and the stria vascularis and spiral ligament were picked away from supporting bone at a level slightly above that of the basilar membrane. The specimens were incubated with 0.01 M PBS containing 0.25% Triton-X 100 for 30 min and then incubated with anti-Prestin antibody (Santa Cruz Biotechnology, Santa Cruz, CA) diluted 1:200 overnight at 4 °C. After the specimens were rinsed with 0.01 M PBS, they were incubated with Alexa Fluor 488-conjugated rabbit anti-goat IgG (Molecular Probes Inc.) diluted 1 : 1000 and Alexa Fluor 568 phalloidin. The images were obtained using a confocal laser scanning microscope (LSM5 Pascal). The outer hair cells were counted as lost if the hair bundles and the expression of Prestin (Belyantseva *et al.* 2000; Zheng *et al.* 2000) could not be observed. The inner hair cells were counted as lost if the hair bundles and the cuticular plate could not be observed.

Scanning electron microscopy

After being perfused with 0.1 M PB containing 4% PFA, mouse temporal bones were removed and immersed in 0.1 M PB containing 4% PFA and 2% glutaraldehyde. The cochleae were processed using the osmium tetrahydrate-thiocarbohydrazide method (Hunter-Duvar 1978). The specimens were finally dehydrated and dried in a critical point dryer. We observed specimens of four *Vlgr1*-mutated mice and specimens of three wild-type littermates and one heterozygous littermate at P0, specimens of three *Vlgr1*-mutated mice and specimens of two wild-type and two heterozygous littermates at P4, specimens of three *Vlgr1*-mutated mice and specimens of five of their heterozygous littermates at P8, specimens of four *Vlgr1*-mutated mice and specimens of three of their heterozygous littermates at P15, and specimens of three *Vlgr1*-mutated mice and specimens of three of their heterozygous littermates at 2 months. The low-magnification scanning electron microscopic images were obtained using the scanning electron microscope S-450 (Hitachi, Tokyo Japan) at 3000× magnification. The hair bundles were analyzed in the low-magnification images. The hair bundles were classified as abnormal if the direction of the hair bundles was shifted by more than approximately 30 degrees from the striamodiolus line, the difference of the length of two sides of the hair bundles was over 50%, or alignments of stereocilia were not in line.

Transmission electron microscopy

After being perfused with 0.1 M PB containing 4% PFA, mouse temporal bones were removed and immersed in 0.1 M PB containing 4% PFA and 2% glutaraldehyde. The specimens were post-fixed

for 90 min in 1% OsO_4, and then dehydrated with ethanol, equilibrated in propylene oxide, and embedded in Durcupan ACM resin (Sigma-Aldrich). To visualize links between stereocilia, Ruthenium Red staining was performed (Goodyear *et al.* 2005). Ultrathin sections were cut and mounted on Formvar-coated single slot grids. Contrast in the specimens was developed with uranyl acetate and lead citrate. Electron micrographs were obtained at 80 kV. Samples were obtained from three *Vlgr1*-mutated mice and three of their heterozygous littermates at P2 and three *Vlgr1*-mutated mice and three of their heterozygous littermates at P8.

Immunoelectron microscopy

Mouse temporal bones were removed and immersed in 0.1 M PB (pH 7.2) containing 4% PFA and 0.02% glutaraldehyde. The cochleae were dissected out from the temporal bones and tectorial membranes were removed. After being rinsed with 0.01 M PBS 3 times, the specimens were incubated with the antibody-dilution-buffer for 1 h at room temperature. The specimens were incubated with rabbit anti-Vlgr1 antisera diluted 1 : 100 in the antibody-dilution-buffer overnight at 4 °C. After five rinses with 0.01 M PBS, the specimens were incubated with 10-nm gold-conjugated goat anti-rabbit IgG (BBInternational, Cardiff, UK) diluted 1 : 50 in the antibody-dilution-buffer overnight at 4 °C. After five rinses with 0.01 M PBS, the specimens were incubated with 0.1 M cacodylate buffer (pH 7.4, Nakalai Tesque, Kyoto, Japan), containing 2% glutaraldehyde for 1 h at room temperature. The specimens were washed with 0.1 M cacodylate buffer 3 times and then washed in distilled water 2 times. They were immersed in fresh silver enhancing solution (BBInternational) for 2 min. After being washed in distilled water, the specimens were dehydrated with a graded ethanol series, equilibrated in propylene oxide, and embedded in Durcupan ACM resin. Ultrathin sections were cut and mounted on Formvar-coated single slot grids. Contrast in the specimens was developed with uranyl acetate and lead citrate. Electron micrographs were obtained at 80 kV.

Incubation of cochleae with a chelator of calcium

Cochleae were obtained from four normal mice at P2 and the bony walls of the cochleae were opened. Tectorial membranes of the cochleae were removed in ice cold HBSS(-) (Sigma-Aldrich). One side of the cochlea was incubated in HBSS(-) and the other side of the cochlea was incubated in HBSS(-) containing 5 mM BAPTA (Sigma-Aldrich) for 1hour at 37 °C. After the incubation, the cochleae were subjected to immunohistochemical analysis as described above.

ABR threshold measurements

The auditory evoked response was recorded with stainless steel needle electrodes inserted subcutaneously into the vertex (active), both of the retroaulicular regions (inactive) and the opposite thigh (ground). The stimulus sound in peak equivalent sound pressure level (peSPL) of tone pips with 0.1-ms slope, 1-ms duration, 70-ms repeat interval with 5.6, 8, 12, 18, 24 kHz frequencies were given by free field in an electrically shielded room. A microcomputer (ER-2104, GE Marquet) was used to analyze the response. Auditory thresholds were obtained for each stimulus by varying the stimulus at 5-dB steps up and down to identify the lowest level at which an ABR pattern could be recognized.

For measurements for postnatal 3-week-old mice, the mice were stimulated with sine waves at 8 kHz frequency with a duration of 0.3 ms using a sound stimulator (DA-502AM, Dana Japan, Japan). The signals were filtered with a band pass between 0.5 and 3 kHz.

Distortion product oto-acoustic emission (DPOAE)

In order to test the function of outer hair cells (Schrott *et al.* 1991), DPOAEs were obtained using a DPOAE measurement device DP-2000 with CUBEDIS v.2.43 software (Mimosa Acoustics). All mice were anaesthetized with ketamine and xylazine at concentrations of 100 and 10 mg/kg, respectively, via intraperitoneal injection and fixed to stereotaxic head gear (SR-5N, Narishige) with a stereotaxic micromanipulator (SM-15, Narishige) supplemented with a DPOAE probe with an attached plastic ear tip containing three sound tubes leading from two loudspeakers and a miniature microphone. This ear tip was inserted into the mouse external auditory canal using the micromanipulator. The primary tone levels L1 and L2 were adjusted as follows: L1 − L2 = 10 dB SPL, L2 = 5 to 55 dB SPL. Their frequency ratio f_2/f_1 was fixed at 1.25 with f_2 = 16, 12, 10, 8, 6, 4 kHz for standard measurements.

Rota-rod test

Mice were subjected to trials on a Rota-rod treadmill (Stoelting Co, Wood Dale, IL). They were tested 3 times per day for three consecutive days on a rod that was accelerated from 4 to 40 rpm. On the final day, the latency to fall from the rod was recorded, and the longest latency was taken as the result.

Statistical analysis

To analyze the duration in the Rota-rod test of *Vlgr1*-mutated mice, we used Student's *t*-test. To analyze the ratio of normal hair bundles of *Vlgr1*-mutated mice and the viability of hair cells of *Vlgr1*-mutated mice, we used the 2-sample test for equality of proportions using Fisher's exact test.

Acknowledgements

We thank H. Yoshikawa and H. Miyagoshi for technical assistance and T. Taniguchi for secretarial assistance, and K. Ando, S. Morikubo, C. Kubota, for helpful discussions. E14-1 ES cells were a generous gift from T. Komori (Nagasaki University, Nagasaki, Japan). Anti-GFP antisera were a generous gift from N. Tamamaki (Kumamoto University, Kumamoto, Japan). This work was supported in part by the Project Allocation Fund and Competitive Allocation Fund of University of Fukui, the 21st Century COE program (Biomedical Imaging Technology Integration Program), a grant-in-aid for scientific research from the Ministry of Education, Culture, Sports, Science and Technology of Japan, Uehara Memorial Foundation and Senri Life Science Foundation.

References

Abe, J., Fukuzawa, T. & Hirose, S. (2002) Cleavage of Ig-Hepta at a "SEA" module and at a conserved G protein-coupled receptor proteolytic site. *J. Biol. Chem.* **277**, 23391–23398.

Ahmed, Z.M., Riazuddin, S., Ahmad, J., Bernstein, S.L., Guo, Y., Sabar, M.F., Sieving, P., Riazuddin, S., Griffith, A.J., Friedman, T.B., Belyantseva, I.A. & Wilcox, E.R. (2003) Localization of the USH1F gene product protocadherin 15 in hair cell stereocilia provided evidence that this protein also directly participates in stereocilia adhesion. *Hum. Mol. Genet.* **12**, 3215–3223.

Alford, B.R. & Ruben, R.J. (1963) Physiological, behavioral and anatomical correlates of the development of hearing in the mouse. *Ann. Otol. Rhinol. Laryngol.* **72**, 237–247.

Belyantseva, I.A., Adler, H.J., Curi, R., Frolenkov, G.I. & Kachar, B. (2000) Expression and localization of prestin and the sugar transporter GLUT-5 during development of electromotility in cochlear outer hair cells. *J. Neurosci.* **20**, RC116.

Bermingham, N.A., Hassen, B.A., Price, S.D., Vollrath, M.A., Ben-Arie, N., Eatock, R.A., Bellen, H.J., Lysakowski, A. & Zoghbi, H.Y. (1999) Math1: an essential gene for the generation of inner ear hair cells. *Science* **284**, 1837–1841.

Bitner-Glindzicz, M. (2002) Hereditary deafness and phenotyping in humans. *Br. Med. Bull.* **63**, 73–94.

Bolz, H., von Brederlow, B., Ramirez, A., Bryda, E.C., Kutsche, K., Nothwang, H.G., Seeliger, M., del C-Salcedo Cabrera, M., Vila, M.C., Molina, O.P., Gal, A. & Kubisch, C. (2001) Mutation of *CDH23*, encoding a new member of the cadherin gene family, causes Usher syndrome type 1D. *Nat. Genet.* **27**, 108–112.

Cremers, C.W.R.J. & Delleman, W.J.W. (1988) Usher's syndrome, temporal bone pathology. *Int. J. Pediatr. Otorhinolaryngol.* **16**, 23–30.

Denk, W., Holt, J.R., Shepherd, G.M.G. & Corey, D.P. (1995) Calcium imaging of single stereocilia in hair cells: localization of transduction channels at both ends of tip links. *Neuron* **15**, 1311–1321.

Forge, A., Souter, M. & Denman-Johnson, K. (1997) Structural development of sensory cells in the ear. *Semin. Cell Dev. Biol.* **8**, 225–237.

Frolenkov, G.I., Beyantseva, I.A., Friedman, T.B. & Griffith, A.J. (2004) Genetic insights into the morphogenesis of inner ear hair cells. *Nat. Rev. Genet.* **5**, 489–498.

Goodyear, R.J., Marcotti, W., Kros, C.J. & Richardson, G.P. (2005) Development and properties of stereociliary link types in hair cells of the mouse cochlea. *J. Comp. Neurol.* **485**, 75–85.

Goodyear, R. & Richardson, G. (1999) The ankle-link antigen: an epitope sensitive to calcium chelation associated with the hair-cell surface and the calycal processes of photoreceptors. *J. Neurosci.* **19**, 3761–3772.

Hone, S.W. & Smith, R.J.H. (2001) Genetics of hearing impairment. *Semin. Neonatol.* **6**, 531–541.

Hunter-Duvar, I.M. (1978) A technique for preparation of cochlear specimens for assessment with the scanning electron microscope. *Acta Otolarungol. Suppl.* **351**, 3–23.

Johnson, K.R., Zheng, Q.Y. & Erway, L.C. (2000) A major gene affecting hearing loss is common at least ten inbred strains of mice. *Genomics* **70**, 171–180.

Johnson, K.R., Zheng, Q.Y., Weston, M.D., Ptacek, L.J. & Noben-Trauth, K. (2005) The $Mass1^{Frings}$ mutation underlies early onset hearing impairment in BUB/BnJ mice, a model for the auditory pathology of Usher syndrome IIC. *Genomics* **85**, 582–590.

Kaltenbach, J.A., Falzarano, P.R. & Simpson, T.H. (1994) Postnatal development of the hamster cochlea. II. Growth and differentiation of stereocilia bundles. *J. Comp. Neurol.* **350**, 187–198.

Keats, B.J. & Corney, D.P. (1999) The Usher syndromes. *Am. J. Med. Genet.* **89**, 158–166.

Markand, O.N. (1994) Brainstem auditory evoked potentials. *J. Clin. Neurophysiol.* **11**, 319–342.

McGee, J., Goodyear, R.J., McMillan, D.R., Stauffer, E.A., Holt, J.R., Locke, K.G., Birch, D.G., Legan, P.K., White, P.C., Walsh, E.J. & Richardson, G.P. (2006) The very large G-protein-coupled receptor VLGR1: a component of the ankle link complex required for the normal development of auditory hair bundles. *J. Neurosci.* **26**, 6543–6453.

McMillan, D.R., Kayes-Wandover, K.M., Richardson, J.A. & White, P. (2002) Very large G protein-coupled receptor-1, the largest known cell surface protein, is highly expressed in the developing central nervous system. *J. Biol. Chem.* **227**, 785–792.

McMillan, D.R. & White, P.C. (2004) Loss of the transmembrane and cytoplasmic domains of the very large G-protein-coupled receptor-1 (VLGR1 or Mass1) causes audiogenic seizures in mice. *Mol. Cell. Neurosci.* **26**, 322–329.

Nance, W.E. (2003) The genetics of deafness. *Ment. Retard. Dev. Disabil. Res. Rev.* **9**, 109–119.

Noben-Trauth, K., Zheng, Q.Y. & Johnson, K.R. (2003) Association of cadherin 23 with polygenic inheritance and genetic modification of sensorineural hearing loss. *Nat. Genet.* **35**, 21–23.

Reiners, J., van Wijk, E., Märker, T., Zimmermann, U., Jürgens, K., te Brinke, H., Overlack, N., Roepman, R., Knipper, M., Kremer, H. & Wolfrum, U. (2005) Scaffold protein harmonin (USH1C) provides molecular links between Usher syndrome type 1 and type 2. *Hum. Mol. Genet.* **14**, 3933–3943.

Ryan, A. & Dallos, P. (1975) Effect of absence of cochlear outer hair cells on behavioural auditory threshold. *Nature* **253**, 44–46.

Schrott, A., Puel, J.-L. & Rebillard, G. (1991) Cochlear origin of $2f_1$-f_2 distortion products assessed by using 2 types of mutant mice. *Hear. Res.* **52**, 245–254.

Schwarz, E.M. & Benzar, S. (1997) *Calx*, a Na-Ca exchanger gene of *Drosophila melanogaster*. *Proc. Natl. Acad. Sci. USA* **94**, 10249–10254.

Skradski, S.L., Clark, A.M., Jinag, H., White, H.S., Fu, Y.-H. & Ptácek, L.J. (2001) A novel gene causing a mendelian audiogenic mouse epilepsy. *Neuron* **31**, 537–544.

Tamamaki, N., Nakamura, K., Furuta, T., Asamoto, K. & Kaneko, T. (2000) Neurons in Golgi-stain-like images revealed by GFP-adenovirus infection *in vivo*. *Neurosci. Res.* **38**, 231–236.

Wagenaar, M., Schuknecht, H., Nadol, J., Jr., Benraad-van Rens, M., Pieke-Dahl, S., Kimberling, W. & Cremers, C. (2000) Histopathological features of the temporal bone in Usher syndrome type I. *Arch. Otolaryngol. Head Neck Surg.* **126**, 1018–1023.

Weston, M.D., Luijendijk, M.W.J., Humphrey, K.D., Möller, C. & Kimberling, W.J. (2004) Mutations in the VLGR1 gene

implicate G-protein signaling in the pathogenesis of Usher syndrome type II. *Am. J. Hum. Genet.* **74**, 357–366.

van Wijk, E., van der Zwaag, B., Peters, T., Zimmermann, U., te Brinke, H., Kersten, F.F.J., Märker, T., Aller, E., Hoefsloot, L.H., Cremers, C.W.R.J., Cremers, F.P.M., Wolfrum, U., Knipper, M., Roepman, R. & Kremer, H. (2006) The *DFNB31* gene product whirlin connects to the Usher protein network in the cochlea and retina by direct association with USH2A and VLGR1. *Hum. Mol. Genet.* **15**, 751–765.

Yagi, H., Deguchi, K., Aono, A., Tani, Y., Kishimoto, T. & Komori, T. (1998) Growth disturbance in fetal liver hematopoiesis of Mll-mutant mice. *Blood* **92**, 108–117.

Yagi, H., Takamura, Y., Yoneda, T., Konno, D., Akagi, Y., Yoshida, K. & Sato, M. (2005) *Vlgr1* knockout mice show audiogenic seizure susceptibility. *J. Neurochem.* **92**, 191–202.

Yagi, H., Yoshida, K., Yoshikawa, H. & Sato, M. (2003) Disruption of neurepin resulted in high susceptibility to audiogenic seizures. *Soc. Neurosci. Abstr.* **33**, 533.20.

Yoshida, N. & Liberman, M.C. (1999) Stereociliary anomaly in the guinea pig: effects of hair bundles rotation on cochlear sensitivity. *Hear. Res.* **131**, 29–38.

Zheng, J., Shen, W., He, D.Z., Long, K.B., Madison, L.D. & Dallos, P. (2000) Prestin is the motor protein of cochlear outer hair cells. *Nature* **405**, 149–155.

Zine, A. & Romand, R. (1996) Development of the auditory receptors of the rat: a SEM study. *Brain Res.* **721**, 49–58.

Received: 17 June 2006
Accepted: 13 November 2006